

# Deep Tile Coder: an Efficient Sparse Representation Learning Approach with applications in Reinforcement Learning

Yangchen Pan

Department of Computing Science, University of Alberta  
pan6@ualberta.ca

## ABSTRACT

Representation learning is critical to the success of modern large-scale reinforcement learning systems. Previous works show that sparse representation can effectively reduce catastrophic interference and hence provide relatively stable and consistent bootstrap targets when training reinforcement learning algorithms. Tile coding is a well-known sparse feature generation method in reinforcement learning. However, its application is largely restricted to small, low dimensional domains, as its computational and memory requirement grows exponentially as dimension increases. This paper proposes a simple and novel tile coding operation—deep tile coder, which adapts tile coding into deep learning setting, and can be easily scaled to high dimensional problems. The key distinction of our method with previous sparse representation learning method is that, we generate sparse feature by construction, while most previous works focus on designing regularization techniques. We are able to theoretically guarantee sparsity and importantly, our method ensures sparsity from the beginning of learning, without the need of tuning regularization weight. Furthermore, our approach maps from low dimension feature space to high dimension sparse feature space without introducing any additional training parameters. Our empirical demonstration covers classic discrete action control and Mujoco continuous robotics control problems. We show that reinforcement learning algorithms equipped with our deep tile coder achieves superior performance. To our best knowledge, our work is the first to demonstrate successful application of sparse representation learning method in online deep reinforcement learning algorithms for challenging tasks without using a target network.

## KEYWORDS

tile coding; reinforcement learning; deep neural networks; representation learning

## 1 INTRODUCTION

Representation learning (RL) plays a significant role in learning efficiency of large machine learning systems. Particularly, the performance of RL agents in function approximation setting can be largely affected by the quality of the representation [6, 7, 15, 20, 23, 24, 41]. One reason is that many RL algorithms require to use the training targets which typically involves bootstrapping estimates from the function approximator itself. This imposes a strong requirement of the representation’s robustness. As pointed out by several previous works [10, 11, 23, 27], the desired properties of a good

representation at least include: 1) reducing catastrophic interference, and 2) preventing forgetting. Learning sparse representation is a promising direction to achieve the two properties, as updated parameters are likely to only have local effect, i.e., a small part of the function domain can get affected. Besides, encouraging sparsity has some other benefits. For example, it provides a way to identify interesting features, since only a few entries in a feature vector can be activated and they have to be informative to express concerned quantities. From another perspective, sparse feature is more likely to be linear independent [8] than dense one. Traditional machine learning community has been actively studying sparse feature learning, including radial basis functions, distributed representation [2, 16, 29, 31], and tile coding encouraged by reinforcement learning research [36, 38, 46]. Incremental sparse feature learning methods are typically formulated as a matrix factorization problem [20, 25, 26].

It should be noted that, in reinforcement learning, although several works [20, 23, 30] have shown the potential benefits of using sparse feature, to our best knowledge, no existed work utilizes sparse feature to solve challenging tasks. It is because that: first, some methods are computationally too expensive to be used in an incremental manner for high dimensional problems; second, many sparse feature learning algorithms themselves are difficult optimization problems and are therefore too complex to be adapted into online reinforcement learning setting.

In order to solve challenging RL problems, deep neural networks are typically used as function approximators [28, 34]. Arguably, one of the most important and popular techniques for successfully training a deep RL algorithm is to use a target network, i.e. a separate slowly-updating network used for computing bootstrap target [28], which is inspired by neural fitted Q iteration [32]. Such technique, however, can largely slower down the learning progress as the updated information is not used immediately when computing the target [11, 23]. Previous works by Liu et al. [23] suggest that sparse representation is a promising direction for removing the need of using a target network. Liu et al. [23] empirically studies the utility of sparse feature in RL problems and proposes a regularization technique for learning sparse feature. However, their proposed strategy requires to pretrain the neural network and does not enable online reinforcement learning for control problems. Rafati and Noelle [30] suggests that sparse feature can reduce the chance of failure of a RL algorithm by reducing catastrophic interference and provides some empirical evidence.

This paper proposes deep tile coder, inspired by tile coding which is well-known in RL problems, and is typically used in linear function approximation setting on small domains [36, 38]. Our method leverages the power of a neural network and can be easily scaled

*Preprint. Under review., 2020*

© 2020 International Foundation for Autonomous Agents and Multiagent Systems (www.ifaamas.org). All rights reserved.

<https://doi.org/doi>

to high dimensional problems. We develop a differentiable tile coding method and hence it is compatible with backpropagation algorithms. Our deep tile coder is general enough to be used in any deep learning algorithms. In addition, our method does not introduce additional training parameters in the process of generating high dimensional sparse features, and hence can be naturally scaled to extremely high sparse feature dimensions. We conduct rigorous experiments to empirically demonstrate the utility of our algorithm on a variety of challenging reinforcement learning problems, ranging from benchmark discrete control to continuous robotics control.

*Notations.* We use bold letter for vectors ( $\mathbf{x}$ ) and bold capital for matrix  $\mathbf{X}$ . Subscript of a vector indicates a scalar at the corresponding location, i.e.  $\mathbf{x}_i$  is the  $i$ th element in the vector.  $[d]$  indicates the set of integers  $\{1, 2, \dots, d\}$ .

## 2 BACKGROUND

In this section, we briefly review tile coding, which inspires our Deep Tile Coder (DTC) method introduced in Section 3. Then we review some background in reinforcement learning and highlight some particular challenges in deep RL algorithms, as it is the main empirical demonstration in our work.

### 2.1 Tile coding

Tile coding<sup>1</sup> is a well-known sparse feature generation method in reinforcement learning [33, 37, 38] and it works as following. Suppose our sample is a scalar  $s \in [0, 1]$  and we intend to convert it to a sparse feature vector. Tile coding specifies a set of tiling  $C$ ,  $|C| = d$ . Each of these tilings has length 1 and the  $i$ th tiling can be denoted as a segment  $[\epsilon_i, \epsilon_i + 1]$  where  $\epsilon_i$  is called the offset value and is typically much smaller than the segment length 1. Then we specify the number of tiles  $k$ , which can be thought of as the resolution of the discretization on each of these segments/tilings. In Figure 1, we show two tilings which can be denoted as two segments  $[0, 1]$ ,  $[0.05, 1.05]$  (i.e.  $|C| = d = 2$ ,  $\epsilon_1 = 0$ ,  $\epsilon_2 = 0.05$ ). Each tiling has 4 tiles ( $k = 4$ ), meaning that we discretize each of the segment into 4 small intervals each of which has length 0.25:  $[0, 0.25]$ ,  $[0.25, 0.5]$ ,  $[0.5, 0.75]$ ,  $[0.75, 1.0]$ . The scalar  $s$  hits second tile on both tilings which gives  $(0, 1, 0, 0)$ ,  $(0, 1, 0, 0)$  respectively, and hence it can be coded by concatenating the two vectors:  $(0, 1, 0, 0, 0, 1, 0, 0)$ .

A nice property of tile coding is that, with multiple tilings, we likely increase the generalization power of our tile coded feature. To see why, consider Figure 1 again and assume that we only use the tiling 1 for coding. Then the two inputs  $s \mapsto (0, 1, 0, 0)$ ,  $s' \mapsto (0, 0, 1, 0)$  do not share any information. However, with two tilings, benefiting from the offset value  $\epsilon_1$ , the two inputs  $s, s'$  hit the same tile on the second tiling, from which they can share the same weight unit in learning tasks.

In general, given a scalar  $\forall s \in [0, 1]$  and an arbitrarily fixed  $\forall i \in [d]$ ,  $s$  must fall into at least one of the intervals in  $[\epsilon_i, \epsilon_i + 1]$ .<sup>2</sup> As a result, on  $[\epsilon_i, \epsilon_i + 1]$ , we can define a  $k$  dimensional binary

<sup>1</sup>We refer readers to <http://www.incompleteideas.net/tiles.html> for software and specific usage examples, and to <https://medium.com/criteo-labs/tile-coding-an-efficient-sparse-coding-method-for-real-valued-data-e787eddf630a> for nice and more specific explanations.

<sup>2</sup>At most two if hits on the middle between two tiles, depending on implementation.

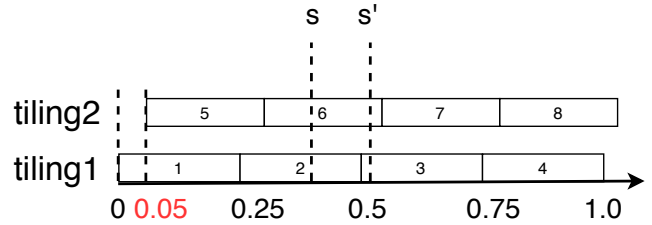


**Figure 1: Tile coding: map a scalar to 8 dimensional binary vector. For example,  $s$  hits second tile on both tilings which gives  $(0, 1, 0, 0)$ ,  $(0, 1, 0, 0)$  respectively. Concatenating the two vectors:  $s \mapsto (0, 1, 0, 0, 0, 1, 0, 0)$ . Similarly,  $s' \mapsto (0, 0, 1, 0, 0, 1, 0, 0)$ .**

vector where each element indicates whether  $s$  falls into the corresponding interval or not. By concatenating all  $|C| = d$  such vectors, we acquire a sparse feature representation for our scalar input  $s$  in the space  $\{0, 1\}^{dk}$ , and there are at most  $d$  nonzero entries in this concatenated vector. One can see that tile coding has the nice property that the sparsity can be guaranteed by choosing appropriate parameter setting.

This procedure generalizes to high dimensional input  $s \in \mathbb{R}^d$ , in which case each tiling in  $C$  becomes a high dimensional object. For example, when  $s \in \mathbb{R}^2$ , we can define each tiling as a square  $[\epsilon_i, \epsilon_i + 1]^2$ ,  $i \in [d]$  with  $4 \times 4 = 16$  tiles on it. Then, given an input  $s$ , we identify the tile hit by  $s$ . Then a 16 dimensional binary vector can be defined on each square and concatenating all those binary vectors gives us a  $16 \times d$  dimensional binary vector with at most  $d$  nonzero entries. One can see that, the computational and memory cost of tile coding grows exponentially as the input dimension increases.

If we know the two elements in  $s$  are always independent, then it is reasonable to tile code them independently and concatenate the corresponding sparse binary vectors. Sutton [37] demonstrates such usage of tile coding by choosing subsets of input variables and tile code those lower dimensional input vectors independently. Such strategy requires significant engineering or preprocessing based on domain knowledge as dependency among input variables is usually unknown [1]. Furthermore, numerous combinations may be needed for tile coding in high dimensional case.

In section 3, we introduce our deep tile coder which takes advantage of a deep neural network to learn a hidden representation, and we design a differentiable tile coding operation to generate sparse feature from the hidden representation without introducing additional training parameters. The differentiability of deep tile coder allows it to be used in backpropagation algorithms when training neural networks. Similar to the vanilla tile coding, the sparsity can be guaranteed for deep tile coder.

### 2.2 Reinforcement Learning

Reinforcement learning is typically formulated within the discounted Markov Decision Process (MDP) framework [38, 40]. A discounted MDP is described by a tuple  $(\mathcal{S}, \mathcal{A}, \mathbb{P}, R, \gamma)$ , where  $\mathcal{S}$  is the state space,  $\mathcal{A}$  is the action space,  $\mathbb{P}$  is the transition probability kernel,  $R$  is the reward function, and  $\gamma \in [0, 1]$  is the discount factor.

At each time step  $t = 1, 2, \dots$ , the agent observes a state  $\mathbf{s}_t \in \mathcal{S}$  and takes an action  $a_t \in \mathcal{A}$ . Then the environment transits to the next state according to the transition probability distribution, i.e.,  $\mathbf{s}_{t+1} \sim \mathbb{P}(\cdot | \mathbf{s}_t, a_t)$ , and the agent receives a scalar reward  $r_{t+1} \in \mathbb{R}$  according to the reward function  $R : \mathcal{S} \times \mathcal{A} \times \mathcal{S} \rightarrow \mathbb{R}$ . A policy is a mapping from a state to an action (distribution)  $\pi : \mathcal{S} \times \mathcal{A} \rightarrow [0, 1]$ . For a given state-action pair  $(\mathbf{s}, a)$ , the action-value function under policy  $\pi$  is defined as  $Q_\pi(\mathbf{s}, a) = \mathbb{E}[G_t | \mathbf{S}_t = \mathbf{s}, A_t = a; A_{t+1:\infty} \sim \pi]$  where  $G_t \stackrel{\text{def}}{=} \sum_{t=0}^{\infty} \gamma^t R(\mathbf{s}_t, a_t, \mathbf{s}_{t+1})$  is the return of a sequence of transitions  $\mathbf{s}_0, a_0, \mathbf{s}_1, a_1, \dots$  by following the policy  $\pi$ .

In control setting, the goal of an agent is to find an optimal policy  $\pi^*$  such that some performance measure can be optimized. Policy gradient methods typically use the mean reward or initial state value objective and directly perform gradient ascent with respect to (w.r.t.) policy parameters [38, 39]. Value-based methods compute the value function (e.g., by performing approximate value iteration and its variants), and obtain the near-optimal policy based on the obtained value function [40, 44]. A popular value-based deep RL algorithm is Deep Q Network (DQN) [28], which updates parameter in Q network by sampling a mini-batch of experiences from a experience replay buffer [22] at each environment time step. That is, we sample a mini-batch of transitions in the form of  $(\mathbf{s}_t, a_t, \mathbf{s}_{t+1}, r_{t+1}, \gamma)$  to update parameter  $\theta$  in  $Q_\theta : \mathcal{S} \times \mathcal{A} \mapsto \mathbb{R}$  by minimizing:

$$(y_t - Q_\theta(\mathbf{s}_t, a_t))^2$$

and  $y_t$  is computed by one-step bootstrap target with a separate target Q network  $Q_{\theta^-} : \mathcal{S} \times \mathcal{A} \mapsto \mathbb{R}$  parameterized by  $\theta^-$ :

$$y_t = \begin{cases} r_{t+1} & \text{if episode ends at } \mathbf{s}_{t+1} \\ r_{t+1} + \gamma \max_{a'} Q_{\theta^-}(\mathbf{s}_{t+1}, a') & \text{o.w.} \end{cases}$$

The target network parameter  $\theta^-$  is updated by copying  $\theta$  periodically. It should be noted that the target network technique is also popular in policy-based approaches, particularly in actor-critic algorithms [13, 14, 19], the target network is frequently used for the purpose of learning a critic. For example, a popular actor-critic continuous control algorithm is deep deterministic policy gradient (DDPG) by Lillicrap et al. [21], which is built upon deterministic policy gradient theorem [35]. Let  $\pi_\psi(\cdot) : \mathcal{S} \rightarrow \mathcal{A}$  be the actor network parameterized by  $\psi$ , and  $Q_\theta(\cdot, \cdot) : \mathcal{S} \times \mathcal{A} \rightarrow \mathbb{R}$  be the critic. The critic  $Q_\theta(\cdot, \cdot)$  is updated with a target network in the similar way as done in DQN except that the maximum action value is computed by using the actor's output action:  $Q_{\theta^-}(\mathbf{s}_{t+1}, \pi_{\psi^-}(\mathbf{s}_{t+1}))$ , where  $\theta^-$ ,  $\psi^-$  are target network parameters of critic, actor respectively.

The target network technique is not in accordance with the spirit of fully-incremental, online reinforcement learning and it can potentially slower down the learning progress [11, 17, 23]. The updated information is not immediately reflected when computing the bootstrap target. However, it is empirically considered as a successful strategy for stabilizing the training process [28, 43, 48]. In Section 4, we empirically demonstrate that DQN with our deep tile coder can significantly outperform vanilla DQN, no matter we use a target network or not.

### 3 DEEP TILE CODER

In this section, we first introduce our main approach for generating sparse representation called Deep Tile Coder (DTC) in Section 3.1.

Then we provide some simple theoretical guarantee regarding the sparsity of learned sparse representation in Section 3.2. We attach the python code of tensorflow-based [9] implementation in the Appendix 6.1.

#### 3.1 Algorithm description

We leverage the representation power of a neural network and consider the outputs of a hidden layer as conditionally independent; then tile coding can be applied to each individual feature unit and the final sparse feature vector can be acquired by concatenating all of the corresponding onehot vectors. Importantly, in order to conveniently train neural networks by backpropagation algorithms, we develop a differentiable tile coding operation which maps the learned hidden representation to sparse representation and this mapping process does not introduce any additional training parameters. Then the sparse representation can be further used to solve desired tasks such as regression, classification, decoder, etc. (typically through a linear operation). Notice that, considering hidden layer outputs as independent are not new; it has been frequently used in factor analysis [45], mean field approximation for variational inference [4], etc.

Given an input  $\mathbf{s}$ , let  $\mathbf{h}(\mathbf{s}; \theta) \in \mathbb{R}^d$  be some hidden layer whose output values are determined by parameter vector  $\theta$ . We write  $\mathbf{h}$  as shorthand unless clarification is needed. Now we would like to convert  $\mathbf{h}$  to sparse feature vector by deep tile coding. Assume that the layers before  $\mathbf{h}$  are powerful enough to capture the dependencies and hence we can think of each hidden unit  $\mathbf{h}_i$  as independent with each other. Consider first that we use a bounded activation function so we have  $\mathbf{h} \in [l, u]^d$ . For example, choosing sigmoid activation gives  $l = 0, u = 1$ . Given tile width  $\delta$ , we denote a tiling  $\mathbf{c}$  as a  $k$ -dimensional vector (i.e.  $k$  tiles,  $k \geq 1$ ) where the integer  $k = (u - l)/\delta$ :<sup>3</sup>

$$\mathbf{c} \stackrel{\text{def}}{=} (l, l + \delta, l + 2\delta, \dots, u - \delta). \quad (1)$$

Comparing with the tiling introduced in Section 2.1, the above definition of tiling is corresponding to use the cut off points between tiles. One difference with vanilla tile coding is that we consider the offset values of different tilings are the same (i.e.  $\epsilon_i = 0$ ) across tilings, since those offset values are constants. We design the following function  $\phi : \mathbb{R} \mapsto \{0, 1\}^k$  to map a scalar to a onehot vector:

$$\phi(x; \mathbf{c}, \delta) \stackrel{\text{def}}{=} 1 - I_+(\max(\mathbf{c} - x, 0) + \max(x - \delta - \mathbf{c}, 0)) \quad (2)$$

where  $I_+(\cdot)$  is an indicator function which operates on the input element-wise. It returns 1 if the corresponding element is positive and 0 otherwise. Vector  $\mathbf{c}$  minus scalar  $x$  is computed by subtracting  $x$  from each element in  $\mathbf{c}$ . Then we can convert each element  $\mathbf{h}_i$  to a onehot vector through this function.

**REMARK 1.** *We slightly abuse the notion of onehot vector here. The function (2) gives a vector with exactly one nonzero entry except when  $x$  is exactly equal to one of  $\mathbf{c}_i$ ,  $i \in \{2, \dots, k\}$ , in which case, there are two nonzero entries. This means when  $x$  hits the middle of two neighboring tiles, we think that it is activating both tiles. We analyze this in Lemma 1. In the Appendix 6.2, we provide an operation for generating a vector with exactly one nonzero entry and discuss the*

<sup>3</sup>Note that the activation function type,  $\mathbf{c}$  and  $\delta$  are chosen by users, we assume  $\delta$  they are chosen such that  $k$  is an integer.

possibility of using more complicated/general DTC, which may be of independent interest to certain research community.

EXAMPLE 1. Consider that we use a bounded activation function, i.e.  $\mathbf{h} \in [0, 1]^d$ . Let the tile width  $\delta = 0.25$  and the tiling  $\mathbf{c}$  with four tiles has length 1.0 and hence it can be denoted as a vector  $\mathbf{c} = (0, 0.25, 0.5, 0.75)$ . Assume we now want to convert  $\mathbf{h}_1 = 0.3$  to a onehot vector. As  $0.25 < 0.3 < 0.5$ , the desired output onehot vector should be  $(0, 1, 0, 0)$  (i.e. 0.3 hits the second tile on the tiling). We now verify that we can acquire this onehot vector through the above function (2).

$$\max(\mathbf{c} - \mathbf{h}_1, 0) = (0, 0, 0.15, 0.45) \quad (3)$$

$$\max(\mathbf{h}_1 - \delta - \mathbf{c}, 0) = \max(0.05 - \mathbf{c}, 0) \quad (4)$$

$$= (0.05, 0, 0, 0) \quad (5)$$

Then (3)+(5) is:

$$(0.05, 0, 0.15, 0.45),$$

hence,

$$\begin{aligned} 1 - I_+(0.05, 0, 0.15, 0.45) &= 1 - (1, 0, 1, 1) \\ &= (0, 1, 0, 0), \end{aligned}$$

which is the desired result. For  $\mathbf{h}_i, \forall i \in [d]$ , going through the same operation as above gives us  $d$  onehot vectors and the concatenation of these vectors is a  $5d$  dimensional vector with  $d$  nonzero entries.

REMARK 2. Instead of using a binary vector, where the activated unit is 1, we can use another hidden layer to give an activation strength to make it more expressive. That is, we can acquire the final sparse vector by taking product between (2) and a hidden unit from another hidden layer  $\mathbf{a}$ :  $\mathbf{a}_i \phi(\mathbf{h}_i; \mathbf{c}, \delta)$ . Notice that this scalar-vector product does not increase the number of nonzero entries and hence sparsity can be still guaranteed.

It should be noted that, the above  $I_+$  function is problematic for training the neural network with backpropagation algorithm since it has zero derivative everywhere except the non-differentiable point at 0. We now propose to approximate the  $I_+$  function by the following function:

$$I_+(\mathbf{x}) \approx \hat{I}_+(\mathbf{x}; \eta) \stackrel{\text{def}}{=} I(\mathbf{x} \leq \eta) \circ \mathbf{x} + I(\mathbf{x} > \eta) \quad (6)$$

where  $\eta$  is some small constant parameter for controlling the sparsity,  $I(\cdot)$  is an indicator function operates element-wise and returns 1 if the input Boolean variable is true otherwise 0, and  $\circ$  is element-wise product. Note that, the original indicator function  $I_+$  can be acquired by setting  $\eta = 0$ . When  $\eta > 0$ , gradient can be backpropagated through this approximation for all entries which are less or equal than  $\eta$ . Replacing  $I_+$  by  $\hat{I}_+$  in (2), we can approximate the  $\phi$  function as:

$$\hat{\phi}(\mathbf{x}; \mathbf{c}, \delta, \eta) \stackrel{\text{def}}{=} 1 - \hat{I}_+(\max(\mathbf{c} - \mathbf{x}, 0) + \max(\mathbf{x} - \delta - \mathbf{c}, 0); \eta) \quad (7)$$

We summarize the algorithm which maps a vector  $\mathbf{h} \in \mathbb{R}^d$  to a  $dk$ -dimensional sparse vector in Algorithm 1 by using the above function (7). The algorithm takes two input vectors  $\mathbf{h}$  and  $\mathbf{a}$ . The former is used to compute which entry in the sparse vector should be activated, and the latter is used to give a specific activation strength for activated units as discussed in the previous Remark 2. Notice that, our DTC can be plugged into any neural network architecture and be trained with any loss function in an end-to-end manner.

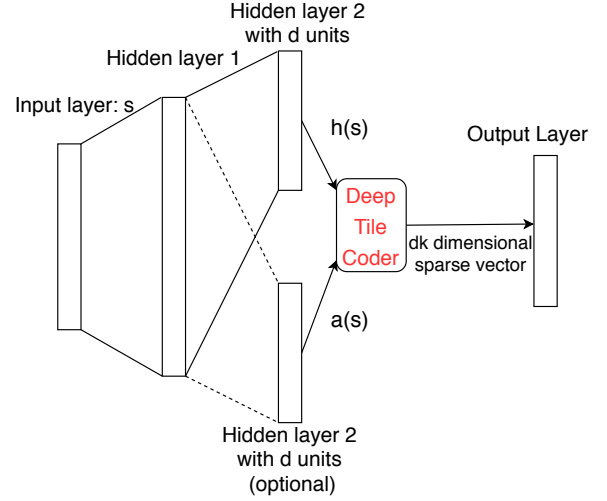


Figure 2: An example of using our DTC algorithm with  $k$  tiles (i.e.  $\mathbf{c} \in \mathbb{R}^k$ ) in a two-hidden-layer neural network. The hidden layer  $\mathbf{h}$  is converted to  $dk$  dimensional sparse feature through DTC.

---

**Algorithm 1** Deep tile coder, denoted as  $\psi : \mathbb{R}^d \times \mathbb{R}^d \mapsto \mathbb{R}^{dk}$

---

Fixed parameters: a  $k$ -dimensional tiling vector  $\mathbf{c} \in \mathbb{R}^k$ , sparsity control parameter  $\eta$   
Input:  $d$ -dimensional hidden layer output  $\mathbf{h} \in \mathbb{R}^d$ ; another  $d$ -dimensional hidden layer output  $\mathbf{a} \in \mathbb{R}^d$ ;  
initialize an empty vector  $\mathbf{r} \leftarrow (\cdot)$   
// Perform the sparse feature mapping operation for each element in  $\mathbf{h}$   
**for**  $i \in [d]$  **do**  
Append  $\mathbf{a}_i \hat{\phi}(\mathbf{h}_i; \mathbf{c}, \delta, \eta) \in \mathbb{R}^k$  to  $\mathbf{r}$   
**output**  $\mathbf{r} \in \mathbb{R}^{kd}$

---

Furthermore, our DTC algorithm itself does not introduce any additional training parameters, in contrast to the regularization-based methods. Figure 2 shows an example of using DTC in a feedforward neural network. The example shows that after sharing the first hidden layer, two-stream second hidden layers are used for computing which tiles to hit and for computing the activation strength respectively. In practice, users can flexibly design the hidden layer for computing activation strength. We provide some suggestions in Appendix 6.1.

REMARK 3. In principle, we need to assume that the hidden units  $\mathbf{h}$  must be bounded. This may limit the generality of the neural network. However, in Section 4.2, we empirically show that an unbounded function can be also used in practice with an additional loss to penalize the out of boundary values.

### 3.2 Theoretical Analysis

We now provide some simple theoretical analysis for our deep tile coding method. The first lemma verifies that the function  $\phi$  indeed



gives the desired onehot vector; the second lemma provides sparsity guarantee for our DTC algorithm.

**LEMMA 1. Onehot vector verification.** *Let the tile width  $\delta \in \mathbb{R}$  be some reasonable value so that  $\mathbf{c}$  is a vector with  $k$  evenly spaced increasing elements as defined in (1). Fixed arbitrary  $x \in [l, u]$ .*

- 1) If  $\mathbf{c}_i < x < \mathbf{c}_{i+1}$  for some  $i \in [k]$  (define the out of boundary value  $\mathbf{c}_{k+1} \stackrel{\text{def}}{=} u$ ), then the function  $\phi(x; \mathbf{c}, \delta)$  gives an onehot vector where the  $i$ th entry is 1;
- 2) If  $x = \mathbf{c}_i$  for some  $i \in \{2, \dots, k\}$ ,  $\phi(x; \mathbf{c}, \delta)$  returns a vector with two nonzero entries at  $(i-1)$ th,  $i$ th positions.

**PROOF.** By assumption, in either case, the first maximum operation in  $\phi$  is

$$\max(\mathbf{c} - x, 0) = (0, 0, \dots, \mathbf{c}_{i+1} - x, \mathbf{c}_{i+2} - x, \dots, \mathbf{c}_k - x).$$

For the second maximum operation,

1) since  $\mathbf{c}_i < x < \mathbf{c}_{i+1}$ ,  $\mathbf{c}_{i-1} < x - \delta < \mathbf{c}_i$ ; and this implies:

$$\max(x - \delta - \mathbf{c}, 0) = (x - \delta - \mathbf{c}_1, x - \delta - \mathbf{c}_2, \dots, x - \delta - \mathbf{c}_{i-1}, 0, 0, \dots, 0)$$

So  $\max(\mathbf{c} - x, 0) + \max(x - \delta - \mathbf{c}, 0)$  has positive entry everywhere except the  $i$ th position. Hence  $I_+(\max(\mathbf{c} - x, 0) + \max(x - \delta - \mathbf{c}, 0))$  gives a vector where every entry is 1 except the  $i$ th entry which is 0. Then  $1 - I_+(\max(\mathbf{c} - x, 0) + \max(x - \delta - \mathbf{c}, 0))$  is a onehot vector where the  $i$ th entry is one.

2) when  $x = \mathbf{c}_i$ ,  $i \in \{2, \dots, k\}$ , then  $\mathbf{c}_{i-1} = x - \delta$  and

$$\max(x - \delta - \mathbf{c}, 0) = (x - \delta - \mathbf{c}_1, x - \delta - \mathbf{c}_2, \dots, x - \delta - \mathbf{c}_{i-2}, 0, 0, \dots, 0).$$

It follows that the vector  $\max(\mathbf{c} - x, 0) + \max(x - \delta - \mathbf{c}, 0)$  has two zero entries at  $i-1$ th and  $i$ th entry, and  $1 - I_+(\max(\mathbf{c} - x, 0) + \max(x - \delta - \mathbf{c}, 0))$  gives us a vector with ones at  $i-1$ th and  $i$ th entry.

Particularly in the second case, when  $x = \mathbf{c}_1$ ,  $\max(x - \delta - \mathbf{c}, 0)$  is a zero vector and  $\max(\mathbf{c} - x, 0)$  is positive everywhere except the first entry, so  $\phi(\cdot)$  still gives a onehot vector where the only nonzero entry is the first entry.  $\square$

**LEMMA 2. Sparsity guarantee.** *Given the sparsity control parameter  $\eta \in [0, u - l]$ , a valid tiling vector  $\mathbf{c}$  as defined in (1), two vectors  $\mathbf{h}, \mathbf{a} \in [l, u]^d$ , the Algorithm 1 returns a vector  $\psi(\mathbf{h}, \mathbf{a}, \mathbf{c}, \eta)$  whose proportion of nonzero entries is at most:*

$$\frac{2 + \min(2\lfloor \frac{\eta}{\delta} \rfloor, k - 2)}{k}$$

**PROOF.** Denote  $x = \mathbf{h}_1$ . Consider  $\mathbf{c}_i < x < \mathbf{c}_{i+1}$  first, since the case  $\mathbf{c}_i = x$ ,  $i \in \{2, \dots, k\}$  simply gives us one more nonzero entry. Similar to the above proof for Lemma 1,

$$\max(\mathbf{c} - x, 0) = (0, 0, \dots, \mathbf{c}_{i+1} - x, \dots, \mathbf{c}_k - x) \quad (8)$$

$$\max(x - \delta - \mathbf{c}, 0) = (x - \delta - \mathbf{c}_1, \dots, x - \delta - \mathbf{c}_{i-1}, 0, 0, \dots, 0), \quad (9)$$

taking the sum of the two equations gives us a vector as following:

$$(x - \delta - \mathbf{c}_1, \dots, x - \delta - \mathbf{c}_{i-1}, 0, \mathbf{c}_{i+1} - x, \mathbf{c}_{i+2} - x, \dots, \mathbf{c}_k - x)$$

We count the number of entries less than  $\eta$  in this vector from the  $i$ th position where the corresponding entry is zero.

First, count number of entries  $\leq \eta$  on the left side of the  $i$ th position. Since the  $i$ th position is zero, which indicates  $x - \delta - \mathbf{c}_i < 0$ , hence  $x - \delta - \mathbf{c}_{i-1} - \delta < 0$  and it follows that  $0 < x - \delta - \mathbf{c}_{i-1} < \delta$ .

Then  $x - \delta - \mathbf{c}_{i-2} = x - \delta - \mathbf{c}_{i-1} + \delta < 2\delta$ . Then the total number of entries  $\leq \eta$  on the left side of the  $i$ th position is at most  $\lfloor \frac{\eta}{\delta} \rfloor$ .

Second, count the number of entries  $\leq \eta$  on the right side of the  $i$ th position. Since  $\mathbf{c}_i - x < 0$ ,  $\mathbf{c}_{i+1} - x = \mathbf{c}_i + \delta - x < \delta$ ,  $\mathbf{c}_{i+2} - x < 2\delta, \dots$ . Hence the maximum number of entries  $\leq \eta$  on the right side of  $i$ th position is  $\lfloor \frac{\eta}{\delta} \rfloor$ .

As a result, taking into consideration the case that  $x = \mathbf{c}_i$ , the number of nonzero entries is at most  $2 + \min(2\lfloor \frac{\eta}{\delta} \rfloor, k - 2)$  by processing a single element in  $\mathbf{h}$  (i.e. a single for loop in Algorithm 1). After the for loop, we would have at most  $d(2 + \min(2\lfloor \frac{\eta}{\delta} \rfloor, k - 2))$  nonzero elements and hence the corresponding proportion of nonzero entries is at most

$$\frac{2 + \min(2\lfloor \frac{\eta}{\delta} \rfloor, k - 2)}{k} \quad \square$$

**REMARK 4.** *Typically  $\eta$  is chosen as some small value. Consider  $\eta = \delta$ . Then even for a tiling with 40 tiles, the proportion of nonzero entries is no more than 10%. As we empirically verify later in Section 4.1, the proportion of nonzero entries is very low. Furthermore, we want to emphasize that DTC achieves sparsity by construction/design instead of learning through some regularization. Hence, sparsity is guaranteed at the beginning of learning.*

## 4 EMPIRICAL DEMONSTRATION IN REINFORCEMENT LEARNING

In this section, we firstly show empirical results on benchmark discrete action domains with extensive runs. Then we demonstrate the utility of our algorithm on challenging Mujoco robotics continuous control domains. The naming rule of the baselines we used is as following.

- **(NoTarget)DQN**: the DQN algorithm with or without using target network respectively.
- **(NoTarget)DQN-DTC**: (NoTarget)DQN equipped with our DTC to acquire sparse feature and an action value is defined as a linear function of the sparse feature.

### 4.1 Discrete control

The purposes of the experiment are: 1) rigorously compare DQN using our DTC with several baselines with extensive runs and sufficient number of training steps to ensure that the algorithm does not diverge in the long term; 2) show that using DTC can significantly improve performance and can learn stably in the sense that it has low standard error across runs; 3) verify the sparsity of the sparse feature obtained by DTC. We use  $32 \times 32$  hidden units on MountainCar, CartPole, Acrobot and use  $128 \times 64$  hidden units on LunarLander as it is a more difficult task. Across all experiments, for DTC setting, we use  $\mathbf{c} = \{-1.0, -0.95, -0.9, \dots, 0.95\}$ ,  $\delta = \eta = 0.05$  and hence number of tiles  $k = 2/0.05 = 40$ . We use  $\tanh$  units for second hidden layer to ensure the feature before DTC is bounded within  $[-1, 1]$ . Note that our DTC maps from a 32-dimensional vector to a  $32 \times \frac{2}{0.05} = 1280$ -dimensional sparse feature for computing action-values (and from 64 to 2560 dimensions on LunarLander domain). In order to ensure fair comparison, for DQN and NoTargetDQN, we sweep over hidden unit types between ReLU, tanh to optimize the algorithms. Furthermore, we test DQN/NoTargetDQN:

**Table 1: Sparsity on different domains**

Sparsity	MCar	CartPole	Acrobot	Lunar
Instance	7.42%	7.46%	7.31%	7.42%
Overlap	3.75%	3.38%	3.05%	3.82%

1) with the same size  $Q$ -network as we have for DTC versions before DTC operation; 2) with a larger  $Q$ -network whose second layer hidden size is the same as sparse feature dimension generated by DTC.

Figure 3 shows the learning curves of different algorithms on benchmark domains from OpenAI [5]: MountainCar (MCar), Cart-Pole, Acrobot, LunarLander (Lunar). From this figure, one can see that: 1) with or without using a target network, DQN with DTC can significantly outperform the version without using DTC; 2) DTC versions have significantly lower standard errors/variances in most of the figures; 3) NoTargetDQN-DTC outperforms DQN-DTC in general, which indicates a potential gain by removing the target network; 4) without using DTC, NoTargetDQN cannot perform well in general, this clearly indicates the utility of sparse feature and coincides with conclusions/conjectures from several previous works [23, 30]; 5) simply by using larger neural network cannot guarantee performance improvement.

Given our DTC setting, Lemma 2 guarantees that the proportion of nonzero entries in our learned feature representation should be no more than 10%. This measure of sparsity is typically called instance sparsity. In below Table 1, one can see that our learned feature has lower proportion of nonzero entries than the upper bound provided by the lemma. Additionally, we report overlap sparsity [10] which is defined as

$$overlap(\psi, \psi') = \frac{\sum_i I(\psi_i \neq 0)I(\psi'_i \neq 0)}{kd}$$

given two sparse vectors  $\psi, \psi'$ . It can be thought of as a measure of the level of representation interference. Low overlap sparsity potentially indicates less feature interference between different input samples. We compute an estimate of sparsity by sampling a mini-batch of samples from experience replay buffer and taking the average of them. The reported numbers in the table are acquired by taking the average of those estimates across 50k training steps. It should be noted that, the sparsity of DTC is achieved by the design of tile coding, i.e. the choice of the number of tiles and  $\eta$ . This explains that the sparsity achieved on each domain is very similar to each other, since we use the same  $\eta$  and number of tiles across all tests.

## 4.2 Continuous control

The purpose of our robotics continuous control experiments is to show that: 1) DTC can work even with unbounded activation function by adding an additional loss for out of boundary values; 2) our sparse feature can be used to solve challenging continuous Mujoco [42] control problems which indicates the practical utility of DTC. To our best knowledge, this is the first time sparse representation learning method is used in an online manner to solve challenging continuous control problems.

In order to use unbounded activation function, we introduce an additional out of boundary loss:

$$\forall \mathbf{s} \in \mathcal{S}, I(|\mathbf{h}(\mathbf{s})| > u) \circ |\mathbf{h}(\mathbf{s})|$$

where  $\mathbf{h}$  indicates the hidden layer right before using DTC and  $u$  is the bound for the tilings. The intuition of this loss is as following. The activation function is unbounded (i.e. linear), but we have to use a bound to do tile coding. Consider that we use a tiling:  $\mathbf{c} = (-u, -u + \delta, -u + 2\delta, \dots, u - \delta)$ . Then we enforce a constraint so that most of the values in  $\mathbf{h}$  should be within the boundary. It should be noted that, for those values which are out of boundary, they do not activate any tile; as a result, the effect of going out of boundary does not increase the density of the representation.

We are able to keep exactly the same DTC setting across all continuous control experiments: we use  $u = 10, \delta = \eta = 0.5$  (i.e. 40 tiles on each tiling, the same as we do for the above discrete control experiments). We use ReLU units for all algorithms except for NoTargetDDPG-DTC, whose second hidden layer activation function is linear (no activation function). Then DTC is applied to this hidden layer to acquire sparse feature and the action value is a linear function of it. Figure 4 shows that our DDPG equipped with DTC can always achieve superior performance than, or at least comparable performance with, vanilla DDPG; while vanilla DDPG without using a target network performs significantly worse than our algorithm on most of the domains. This further verifies the practical effectiveness of using DTC for RL problems.

## 5 DISCUSSION

We propose a novel and simple sparse representation learning method, Deep Tile Coder (DTC), which can efficiently map dense representation to high dimensional sparse representation without introducing additional training parameters. We design a differentiable tile coding operation so that DTC can be conveniently incorporated into any neural network architecture and be trained with any loss function in an end-to-end manner. We empirically study the utility of DTC in RL algorithms on various benchmark domains. Our experimental results show that RL algorithms equipped with DTC is able to learn with lower variance and does not need to use a target network. Our DTC method should be an important step towards fully incremental, online reinforcement learning.

We would like to point out several interesting future directions. First, the complex tile coding as discussed in Appendix 6.2 may have special utility for improving interpretability of deep learning, because defining tilings with different resolutions implicitly forces a neural network to learn finer sensors on those hidden units which are assigned finer resolutions. Second, it is worthy investigating the property of our onehot operation  $\hat{\phi}$  by considering it as a special type of activation function. Note that if the previous hidden layer is linear (without using any activation function), our  $\hat{\phi}$  function can be thought of as a special composition of ReLU which maps a one dimensional scalar to a high dimensional vector.

## 6 APPENDIX

Section 6.1 includes experimental details for reproducible research. Additional discussions regarding deep tile coder is in Section 6.2. Additional experimental results are presented in Section 6.3.

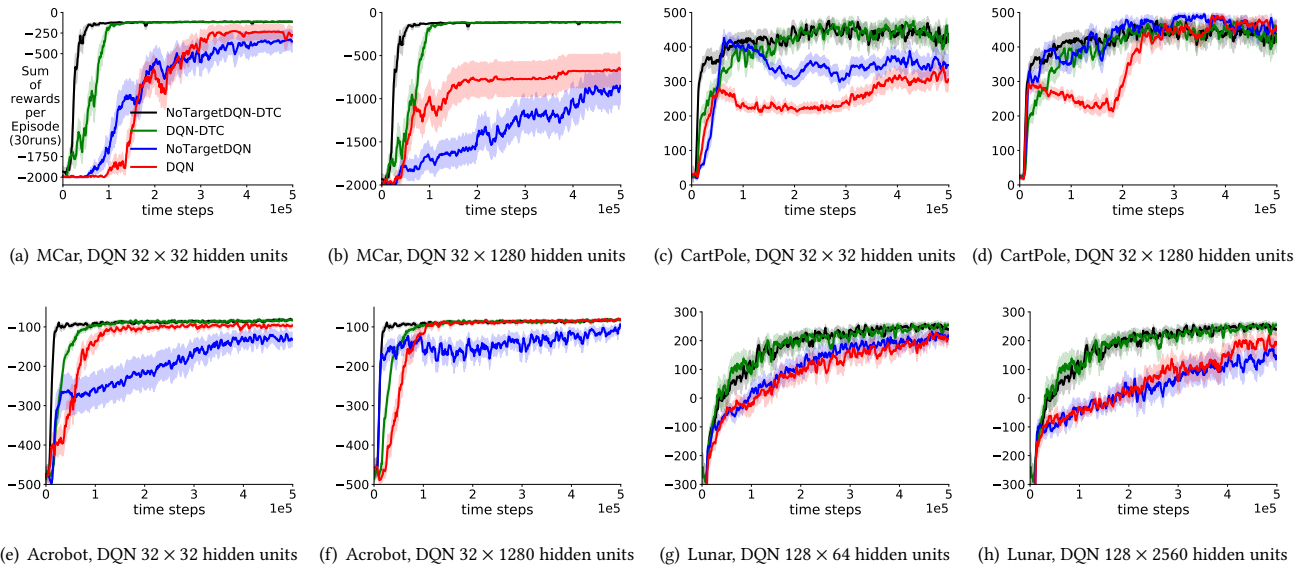


**Figure 3: Evaluation learning curves on MountainCar(MCar), CartPole, Acrobot and LunarLander domains by averaging over 30 random seeds and the shade indicates standard error. The caption of each figure explains the neural network size used by DQN and NoTargetDQN. Note that, to use the same high dimensional feature as our DTC, DQN would introduce much more training parameters (about  $128 \times 2560$  on LunarLander and  $32 \times 1280$  on other domains).**

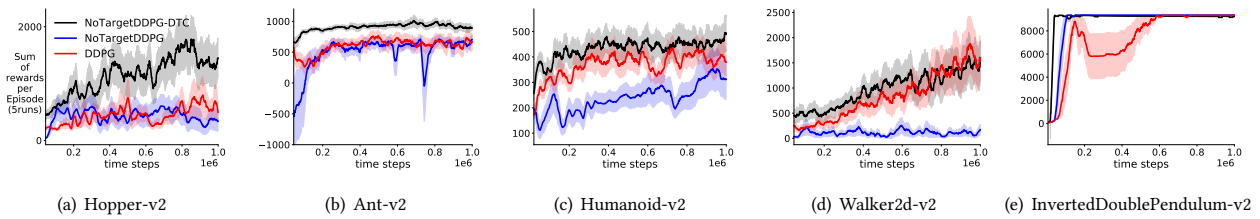


**Figure 4: Evaluation learning curves on several challenging mujoco domains, the results are averaged over 5 random seeds.**

### 6.1 Reproducible Research

We now provide details to reproduce our experimental results.

All discrete action domains are from OpenAI Gym [5] with version 0.14.0. Deep learning implementation is based on tensorflow with version 1.13.0 [9]. We use Adam optimizer [18], Xavier initializer [12], mini-batch size  $b = 64$ , buffer size 100k, and discount rate  $\gamma = 0.99$  across all experiments. All activation functions are ReLU except: the output layer of the  $Q$  value is linear, and the second hidden layer is using tanh for our DTC versions. The output layers were initialized from a uniform distribution  $[-0.003, 0.003]$ .

We set the episode length limit as 2000 for MountainCar and keep all other episode limit as default settings. We use warm-up steps 5000 for populating the experience replay buffer before training. Exploration noise is 0.1 without decaying. For DQN, we use target network moving frequency 1000, i.e. update target network parameters every 1000 training steps. The learning rate is 0.0001 for all algorithms. For each random seed, we evaluate one episode

every 1000 environment time steps and keep a small noise  $\epsilon = 0.05$  when taking action.

On Mujoco domains, we use exactly the same setting as done in the original DDPG paper [21] except that we use a smaller neural network size  $200 \times 100$  relu units for DDPG and NoTargetDDPG. For our algorithm, we use linear second hidden layer before the DTC operation. We use 10,000 warm-up time steps to populate the experience replay buffer and we evaluate each algorithm every 1000 environment time steps and we start evaluation after 40k time steps.

We attach our core part of DTC python code as below.

```
import tensorflow as tf
def Iplus(x, eta):
    return (tf.cast(x <= eta, tf.float32)*x
            + tf.cast(x > eta, tf.float32))
// sparse_dim = dk
def dtc(shoot, strength, c, d, sparse_dim, delta, eta):
    x = tf.reshape(shoot, [-1, d, 1])
```

```

strength = tf.reshape(strength, [-1, d, 1])
sparsevec = (1.0 - Iplus(tf.nn.relu(c - x) \\\
+ tf.nn.relu(x - delta - c), eta)) * strength
return tf.reshape(sparsevec, [-1, sparse_dim])

```

*A brief discussion on the additional activation strength.* We empirically found that on reinforcement learning experiments, there is no clear difference by using or not using a separate activation strength layer. There may be at least two reasons: 1) it is not always necessary to have optimal value function to acquire optimal policy (consider shifting all values by a constant, or add some small perturbations without changing the maximum action); 2) the catastrophic interference problem may matter more than learning an accurate action value function in reinforcement learning setting. However, we do find using activation strength can significantly improve performance in regular machine learning tasks.

## 6.2 More Complicated Tiling Design

As we mentioned in Remark 1, the  $\phi$  function can actually give two nonzero entries and the interpretation is that hitting the middle between two tiles can activate both tiles. For completeness, we also provide the below function which yields a rigorous onehot vector for each tiling and is differentiable:

$$\sum_{i=1}^k I(x = c_i)(1 - I_+(|x - c|)) + (1 - \sum_{i=1}^k I(x = c_i))(1 - I_+(\phi(x; c, \delta)))$$

The idea is quite simple: we basically use an indicator function to judge whether  $x$  is equal to any one of the cut off values on the tiling  $c$  or not. Since we use approximation for the indicator function  $I_+$  which would finally give multiple nonzero entries for each tiling, we do not see the necessity of using the above more complicated function.

*Another type of complex deep tile coding.* Throughout the paper, we use a constant tiling represented by a vector  $c$  for all elements in the vector  $h_i, i \in [d]$ . In fact, we can make this more general by defining tilings with different tiles/resolutions ( $\delta$ s). That is, for each  $h_i$ , we can have a specialized  $c^{(i)}$  and  $\delta_i$ . Then this would give a sparse feature vector with dimension  $\sum_{i=1}^d \frac{c_k^{(i)} + \delta_i - c_1^{(i)}}{\delta_i}$ . This is a way to incorporate human knowledge, as we can assume that some of the feature units should be more important, and providing a finer tiling for those units should force the neural network to learn to make those units informative.

## 6.3 Additional Results on Image Autoencoder

The purpose of the additional experiments is to investigate alternative ways for approximating the indicator function other than  $I_+(x) \approx \hat{I}_+(x; \eta) \stackrel{\text{def}}{=} I(x \leq \eta) \circ x + I(x > \eta)$ . We test another possibility to approximate  $I_+$ . Recall that the function  $I_+$  outputs 1 if input is positive and outputs 0 if zero. As a result, we can also use hyperbolic tangent function  $\tanh$  in the observance of  $\lim_{k \rightarrow \infty} \tanh(kx) = 1$  for any  $x > 0$ . In implementation, we choose some large  $k$  values. Notice that, this way is not as good as previously defined  $\hat{I}_+$  in term of the sparsity control: we can no longer provide rigorous bound for the sparsity. When  $k$  is too small we get dense representation and when  $k$  is too large the  $\tanh$  units can “die”/be inactive.

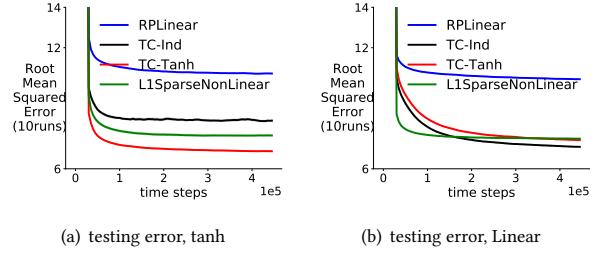


**Figure 5: (a)(b) shows image reconstruction error as a function of the number of mini-batch updates by using tanh and linear for latent feature before DTC operation respectively. For baselines, we use ReLU as we found it works better.**

We conduct some experiments in regular machine learning setting by using a popular image dataset Fashion-Mnist by Xiao et al. [47]. We attempt to learn an autoencoder to reconstruct the images from the Fashion-Mnist dataset. Due to the relatively low dimension of the images in the dataset, we use two layer  $128 \times 128$  fully connected ReLU units to encode an input image to 16-dimensional vector. As for decoding, we include several intuitive/interesting baselines described below which may intrigue researchers from certain areas.

- **RPLinear:** after encoding an image to  $h \in \mathbb{R}^d$ , we use Gaussian random projection [3] (RP) to project it to the same dimension as the sparse feature dimension achieved by our DTC and the recovered image is linear in the projected feature, i.e.  $hP, P \in \mathbb{R}^{d \times dk}$ . This is contrary to a regular usage of random projection, which is typically to reduce feature dimension. The rationality of our design stems from: 1) we can think that the neural network is trying to learn a low dimensional embedding which is compatible with the random projection and 2) similar to our method, this projection process does not introduce additional training parameters.
- **L1SparseNonLinear:** add one more hidden ReLU layer (Non-Linear) after the encoded feature  $h \in \mathbb{R}^d$  and this layer uses  $l_1$  penalty to enforce sparse feature. We sweep regularization weight from  $\{0.0, 0.001, 0.01, 0.1\}$ . Note that this baseline has roughly  $16 \times 40 \times 16$  more training parameters than other algorithms.
- **TC-Ind/Tanh:** use DTC to map  $h$  to sparse feature and the reconstructed image is linear in the sparse feature. Ind and Tanh indicate  $\hat{I}_+$  or  $\tanh$  approximation for  $I_+$  function in DTC respectively.

From Figure 5, we can see that: 1) even though L1SparseNonLinear has larger number of training parameters, our algorithm TC-Ind/Tanh can still significantly outperform it. This highlights the advantage of our DTC method; 2) the utility of using either tanh approximation or  $\hat{I}_+$  seems to be dependent on the activation function type of the low dimensional embedding; 3) a naive random projection to high dimensional space performs significantly worse than our DTC sparse projection.



## REFERENCES

- [1] Marc G. Bellemare, Yavar Naddaf, Joel Veness, and Michael Bowling. 2012. The Arcade Learning Environment: An Evaluation Platform for General Agents. *CoRR* abs/1207.4708 (2012).
- [2] Yoshua Bengio, Aaron Courville, and Pascal Vincent. 2013. Representation learning: A review and new perspectives. *IEEE Transactions on Pattern Analysis and Machine Intelligence* (2013).
- [3] Ella Bingham and Heikki Mannila. 2001. Random Projection in Dimensionality Reduction: Applications to Image and Text Data. In *Proceedings of the Seventh ACM SIGKDD International Conference on Knowledge Discovery and Data Mining*. 245–250.
- [4] David M. Blei, Alp Kucukelbir, and Jon D. McAuliffe. 2016. Variational Inference: A Review for Statisticians. *arXiv e-prints* (2016).
- [5] Greg Brockman, Vicki Cheung, Ludwig Pettersson, Jonas Schneider, John Schulman, Jie Tang, and Wojciech Zaremba. 2016. OpenAI Gym. *CoRR* (2016).
- [6] Hugo Caselles-Dupré, Michaël Garcia Ortiz, and David Filliat. 2018. Continual State Representation Learning for Reinforcement Learning using Generative Replay. *CoRR* abs/1810.03880 (2018).
- [7] Yash Chandak, Georgios Theodorou, James Kostas, Scott M. Jordan, and Philip S. Thomas. 2019. Learning Action Representations for Reinforcement Learning. *CoRR* abs/1902.00183 (2019).
- [8] Thomas M Cover. 1965. Geometrical and Statistical Properties of Systems of Linear Inequalities with Applications in Pattern Recognition. *IEEE Trans. Electronic Computers* (1965).
- [9] Martin Abadi et. al. 2015. TensorFlow: Large-Scale Machine Learning on Heterogeneous Systems. (2015). <http://tensorflow.org/> Software available from tensorflow.org.
- [10] Robert M French. 1991. Using semi-distributed representations to overcome catastrophic forgetting in connectionist networks. In *Annual Cognitive Science Society Conference*.
- [11] Sina Ghassian, Huizhen Yu, Banafsheh Rafiee, and Richard S. Sutton. 2018. Two geometric input transformation methods for fast online reinforcement learning with neural nets. *CoRR* abs/1805.07476 (2018).
- [12] Xavier Glorot and Yoshua Bengio. 2010. Understanding the difficulty of training deep feedforward neural networks. In *Proceedings of the Thirteenth International Conference on Artificial Intelligence and Statistics*. PMLR.
- [13] Tuomas Haarnoja, Aurick Zhou, Pieter Abbeel, and Sergey Levine. 2018. Soft Actor-Critic: Off-Policy Maximum Entropy Deep Reinforcement Learning with a Stochastic Actor. In *Proceedings of the 35th International Conference on Machine Learning (Proceedings of Machine Learning Research)*, Jennifer Dy and Andreas Krause (Eds.). PMLR, 1861–1870.
- [14] Tuomas Haarnoja, Aurick Zhou, Kristian Hartikainen, George Tucker, Sehoon Ha, Jie Tan, Vikash Kumar, Henry Zhu, Abhishek Gupta, Pieter Abbeel, and Sergey Levine. 2018. Soft Actor-Critic Algorithms and Applications. *CoRR* (2018).
- [15] Jacob Rafati Heravi. 2019. *Learning Representations in Reinforcement Learning*. Ph.D. Dissertation. University of California, Merced.
- [16] Pentti Kanerva. 1988. *Sparse Distributed Memory*. MIT Press.
- [17] Seungchan Kim, Kavosh Asadi, Michael Littman, and George Konidaris. 2019. DeepMellow: Removing the Need for a Target Network in Deep Q-Learning. 2733–2739.
- [18] Diederik P Kingma and Jimmy Ba. 2014. Adam: A method for stochastic optimization. *arXiv:1412.6980* (2014).
- [19] Vijaymohan Konda. 2002. Actor-critic Algorithms. (2002).
- [20] Lei Le, Raksha Kumaraswamy, and Martha White. 2017. Learning sparse representations in reinforcement learning with sparse coding. *arXiv:1707.08316* (2017).
- [21] Timothy P. Lillicrap, Jonathan J. Hunt, Alexander Pritzel, Nicolas Heess, Tom Erez, Yuval Tassa, David Silver, and Daan Wierstra. 2016. Continuous control with deep reinforcement learning. In *ICLR*. *CoRR* (2016).
- [22] Long-Ji Lin. 1992. Self-Improving Reactive Agents Based On Reinforcement Learning, Planning and Teaching. *Machine Learning* (1992).
- [23] Vincent Liu, Raksha Kumaraswamy, Lei Le, and Martha White. 2018. The Utility of Sparse Representations for Control in Reinforcement Learning. *CoRR* abs/1811.06626 (2018). [arXiv:1811.06626](https://arxiv.org/abs/1811.06626)
- [24] Sephora Madjheurem and Laura Toni. 2019. Representation Learning on Graphs: A Reinforcement Learning Application. *CoRR* abs/1901.05351 (2019).
- [25] Julien Mairal, Francis Bach, Jean Ponce, and Guillermo Sapiro. 2009. Online dictionary learning for sparse coding. In *International Conference on Machine Learning*.
- [26] Julien Mairal, Francis Bach, Jean Ponce, Guillermo Sapiro, and Andrew Zisserman. 2009. Supervised dictionary learning. In *Advances in Neural Information Processing Systems*.
- [27] Michael McCloskey and Neal J Cohen. 1989. Catastrophic Interference in Connectionist Networks: The Sequential Learning Problem. *Psychology of Learning and Motivation* (1989).
- [28] Volodymyr Mnih, Koray Kavukcuoglu, David Silver, Andrei A Rusu, Joel Veness, Marc G Bellemare, Alex Graves, Martin Riedmiller, Andreas K Fidjeland, Georg Ostrovski, and others. 2015. Human-level control through deep reinforcement learning. *Nature* (2015).
- [29] Randall O’Reilly and Yuko Munakata. 2000. *Computational Explorations in Cognitive Neuroscience Understanding the Mind by Simulating the Brain*. 504 pages.
- [30] Jacob Rafati and David C. Noelle. 2019. Learning sparse representations in reinforcement learning. *arXiv e-prints* (Sep 2019). [arXiv:1909.01575](https://arxiv.org/abs/1909.01575)
- [31] B Ratitch and D Precup. 2004. Sparse distributed memories for on-line value-based reinforcement learning. In *Machine Learning: ECML PKDD*.
- [32] Martin Riedmiller. 2005. Neural fitted Q iteration—first experiences with a data efficient neural reinforcement learning method. In *European Conference on Machine Learning*.
- [33] Alexander Sherstov and Peter Stone. 2005. Function Approximation via Tile Coding: Automating Parameter Choice. 194–205. [https://doi.org/10.1007/11527862\\_14](https://doi.org/10.1007/11527862_14)
- [34] David Silver, Aja Huang, Christopher J. Maddison, Arthur Guez, Laurent Sifre, George van den Driessche, Julian Schrittwieser, Ioannis Antonoglou, Veda Panneershelvam, Marc Lanctot, Sander Dieleman, Dominik Grewe, John Nham, Nal Kalchbrenner, Ilya Sutskever, Timothy Lillicrap, Madeleine Leach, Koray Kavukcuoglu, Thore Graepel, and Demis Hassabis. 2016. Mastering the game of Go with deep neural networks and tree search. *Nature* 529 (2016), 484–503.
- [35] David Silver, Guy Lever, Nicolas Heess, Thomas Degris, Daan Wierstra, and Martin Riedmiller. 2014. Deterministic Policy Gradient Algorithms. In *ICML*. I–387–I–395.
- [36] Richard S Sutton. 1996. Generalization in reinforcement learning: Successful examples using sparse coarse coding. In *Advances in Neural Information Processing Systems*.
- [37] Richard S Sutton. 1996. Generalization in Reinforcement Learning: Successful Examples Using Sparse Coarse Coding. In *Advances in Neural Information Processing Systems 8*. MIT Press, 1038–1044.
- [38] Richard S. Sutton and Andrew G. Barto. 2018. *Reinforcement Learning: An Introduction* (second ed.). The MIT Press.
- [39] R. S. Sutton, David McAllester, Satinder Singh, and Yishay Mansour. 1999. Policy Gradient Methods for Reinforcement Learning with Function Approximation. In *Proceedings of the 12th International Conference on Neural Information Processing Systems*. MIT Press.
- [40] Csaba Szepesvári. 2010. *Algorithms for Reinforcement Learning*. Morgan Claypool Publishers.
- [41] Erik Talvitie and Michael Bowling. 2015. Pairwise Relative Offset Features for Atari 2600 Games. (2015).
- [42] E. Todorov, T. Erez, and Y. Tassa. 2012. MuJoCo: A physics engine for model-based control. In *2012 IEEE/RSJ International Conference on Intelligent Robots and Systems*.
- [43] Hado van Hasselt, Yotam Doron, Florian Strub, Matteo Hessel, Nicolas Sonnerat, and Joseph Modayil. 2018. Deep Reinforcement Learning and the Deadly Triad. *CoRR* (2018). [arXiv:1812.02648](https://arxiv.org/abs/1812.02648)
- [44] Christopher J. C. H. Watkins and Peter Dayan. 1992. Q-learning. *Machine Learning* (1992).
- [45] E. Weber. 1970. Modern Factor Analysis. *Biometrische Zeitschrift* 12, 1 (1970), 67–68.
- [46] Shimon Whiteson, Matthew E. Taylor, and Peter Stone. 2007. Adaptive Tile Coding for Value Function Approximation. (2007).
- [47] Han Xiao, Kashif Rasul, and Roland Vollgraf. 2017. Fashion-MNIST: a Novel Image Dataset for Benchmarking Machine Learning Algorithms. [arXiv:cs.LG/cs.LG/1708.07747](https://arxiv.org/abs/cs.LG/cs.LG/1708.07747)
- [48] Zhuoran Yang, Yuchen Xie, and Zhaoran Wang. 2019. A Theoretical Analysis of Deep Q-Learning. *CoRR* abs/1901.00137 (2019). [arXiv:1901.00137](https://arxiv.org/abs/1901.00137) <http://arxiv.org/abs/1901.00137>